

ORIGINAL RESEARCH ARTICLE

MiR-137 knockdown promotes the osteogenic differentiation of human adipose-derived stem cells via the LSD1/BMP2/SMAD4 signaling network

Xiaohan Ma^{1,2} | Cong Fan^{2,3} | Yuejun Wang^{1,2} | Yangge Du^{1,2} | Yuan Zhu^{1,2} | Hao Liu^{1,2} | Longwei Lv^{1,2} | Yunsong Liu^{1,2} | Yongsheng Zhou^{1,2}

¹Department of Prosthodontics, Peking University School and Hospital of Stomatology, Beijing, China

²Central Laboratory, Peking University School and Hospital of Stomatology, Beijing, China

³Department of General Dentistry II, Peking University School and Hospital of Stomatology, Beijing, China

Correspondence

Cong Fan, MD, Department of General Dentistry II, Peking University School and Hospital of Stomatology, 22 Zhongguancun South Avenue, Haidian, Beijing 100081, China. Email: congcongsherry@sina.com

Funding information

The Project for Culturing Leading Talents in Scientific and Technological Innovation of Beijing, Grant/Award Number: Z171100001117169; National Natural Science Foundation of China, Grant/Award Number: 81700937

Abstract

MicroRNAs are a group of endogenous regulators that participate in several cellular physiological processes. However, the role of miR-137 in the osteogenic differentiation of human adipose-derived stem cells (hASCs) has not been reported. This study verified a general downward trend in miR-137 expression during the osteogenic differentiation of hASCs. MiR-137 knockdown promoted the osteogenesis of hASCs in vitro and in vivo. Mechanistically, inhibition of miR-137 activated the bone morphogenetic protein 2 (BMP2)-mothers against the decapentaplegic homolog 4 (SMAD4) pathway, whereas repressed lysine-specific histone demethylase 1 (LSD1), which was confirmed as a negative regulator of osteogenesis in our previous studies. Furthermore, LSD1 knockdown enhanced the expression of BMP2 and SMAD4, suggesting the coordination of LSD1 in the osteogenic regulation of miR-137. This study indicated that miR-137 negatively regulated the osteogenic differentiation of hASCs via the LSD1/BMP2/SMAD4 signaling network, revealing a new potential therapeutic target of hASC-based bone tissue engineering.

KEYWORDS

human adipose-derived stem cells, LSD1, microRNA, osteogenic differentiation, signaling

1 | INTRODUCTION

Human adipose-derived stem cells (hASCs), as one of the most promising mesenchymal stem cells (MSCs) in bone tissue engineering, are receiving more attention in the clinical treatment of bone-related diseases (Behr, Tang, Germann, Longaker, & Quarto, 2011; Liu et al., 2013; Liu, Zhou, Feng, Ma, & Ni, 2008). However, the rapid and efficient initiation of the osteogenic differentiation of hASCs remains a problem. In addition, lots of molecules and signaling pathways involved in this complicated biological process remain unknown, and considerable research is needed to reveal associated mechanisms and to identify approaches to bone regeneration.

Epigenetics, a spotlight of biological science in recent years, focuses on the gene functions of reversible and heritable variations without DNA sequence changes. It plays a key role in the fate

maintenance and lineage commitment of embryonic stem cells (ESCs) and MSCs. Epigenetic regulation mainly includes DNA methylation, histone modification, and noncoding RNA interference (van Meurs, Boer, Lopez-Delgado, & Riancho, 2019). MicroRNAs (miRNAs) are a class of endogenously and evolutionary conserved small noncoding RNAs that function as posttranscriptional negative regulators by partially or fully complementary binding with the 3' untranslated region (3' UTR) of target messenger RNAs (mRNAs; Ambros, 2004). As novel key regulators of cellular differentiation, several miRNAs, such as miR-21, -34a, -124, -217, and -224, have been reported to regulate the osteogenic differentiation of stem cells (Cai et al., 2019; Dai et al., 2019; Fan et al., 2016; Tang et al., 2019; Yang et al., 2019). MiR-137 has been reported to suppress the proliferation, migration, and invasion of tumor cells in several studies (Chen, Luo, Hu, Li, & Zhang, 2018; Huang, Huang, & Li, 2018; N. Lv et al., 2018; J. Zhang,

He, & Zhang, 2018), but its role in the osteogenic differentiation has never been explored.

Lysine-specific histone demethylase 1 (LSD1), one of the first protein lysine demethylases discovered, specifically catalyzes the demethylation of di- and monomethyl histone 3 lysine 4 and histone 3 lysine 9 (H3K4me1/2 and H3K9me1/2; Perillo et al., 2008; Shi et al., 2004). Our previous studies confirmed that the genetic knockdown or chemical blockade of LSD1 could promote the osteogenic differentiation of MSCs (Ge et al., 2014; Lv et al., 2016). LSD1 is reported to serve as a target gene of miR-137 in neural stem cells, neuroblastoma cells, dorsal root ganglion neurons, non-small-cell lung cancer cells, and endometrial cancer cells (Althoff et al., 2013; Chen et al., 2017; J. Q. Sun et al., 2011; W. Zhang et al., 2018; X. Zhang, Zhang, Yu, Hu, & Hao, 2017), but whether it could also be directly targeted by miR-137 in hASCs still needs to be identified. Therefore, we assumed that miR-137 might affect the osteogenic differentiation of hASCs by regulating LSD1.

As an important member of the bone morphogenetic protein (BMP) family, BMP2 participates in skeletal development, bone formation, and MSCs differentiation (Rosen, 2009; Shu et al., 2011; Wang et al., 2019; Yu, Han, Yan, Lee, & Muneoka, 2012). Drosophila mothers against decapentaplegics (SMADs) are crucial downstream mediators for BMP signal transduction. Mothers against decapentaplegic homolog 4 (SMAD4) can form complexes with other activated SMADs (SMAD1/5/8), and then the heterodimer complexes with diverse transcription factors (coactivators or corepressors) regulate gene expression in the nucleus (Massagué, Seoane, & Wotton, 2005). BMP2 and BMP7 were initially identified by their ability to promote osteogenesis and could share certain receptors in their signaling pathways (Suzuki, Kaneko, Ueno, & Hemmati-Brivanlou, 1997). Moreover, in non-small-cell lung cancer cells, miR-137 inhibits cell migration and invasion by directly targeting 3' UTR of BMP7 (Y. R. Yang et al., 2015), and thus we hypothesized that BMP2 and its downstream gene SMAD4 might be regulated by miR-137 during the osteogenesis of hASCs as well.

In addition, a rhodium (III)-based inhibitor of LSD1 enhanced the amplification of BMP2 gene promoters in prostate cancer cells (Yang et al., 2017), and LSD1 deficiency resulted in increased BMP2 expression in osteoblasts and enhanced bone formation (J. Sun et al., 2018). Therefore, we have reasons to infer that LSD1 might regulate the BMP2-SMAD4 pathway and coregulate the osteogenic differentiation of hASCs together with miR-137.

In this study, we confirmed that miR-137 acted as a negative regulator in the osteogenic differentiation of hASCs via the LSD1/BMP2/SMAD4 signaling network, suggesting that miR-137-targeted gene therapy could supply a new approach to bone regeneration.

2 | MATERIALS AND METHODS

2.1 | Cell culture and osteogenic differentiation

The hASCs of three different donors were obtained from ScienCell Research Laboratory (Carlsbad, CA) and all of the experiments were

repeated in triplicate. These cells were cultured in proliferation medium (PM), composed of Dulbecco's modified Eagle's medium, 10% (v/v) fetal bovine serum, and 1% (v/v) penicillin/streptomycin. For the induction of osteogenic differentiation, the hASCs were cultured in osteogenic medium (OM), consisting of PM, 100 nM dexamethasone, 10 mM β -glycerophosphate, and 0.2 mM L-ascorbic acid. The incubation conditions were set to 5% CO₂ and 100% relative humidity at 37°C.

2.2 | Lentivirus transduction

Recombinant lentiviruses containing green fluorescent protein (GFP)-labeled plasmid vectors were acquired from GenePharma (Suzhou, China). The packaged lentiviruses included miR-137 mimics (miR-137), antisense miR-137 (anti-miR-137), negative control (NC), and antisense LSD1 (anti-LSD1). The hASCs were exposed to the viral supernatant at a multiplicity of infection of 100 with 5 mg/ml polybrene for 12 hr, which was then followed by selection with 1 μ g/ml puromycin (Sigma-Aldrich, St. Louis, MO). To evaluate transduction efficiency, we calculated the percentage of GFP-positive cells under an inverted fluorescence microscope (TE2000-U; Nikon, Tokyo, Japan).

2.3 | Alkaline phosphatase staining and quantification

The hASCs were cultured in PM or OM for 7 day and used for alkaline phosphatase (ALP) staining and the activity assay. ALP staining and quantification were, respectively, performed with an NBT/BCIP staining kit (Beyotime Biotechnology, Shanghai, China) and ALP assay kit (Nanjing Jiancheng Bioengineering Institute, Nanjing, China). The total protein content was measured using the bicinchoninic acid method with a pierce protein assay kit (Thermo Fisher Scientific, Rockford, IL). ALP relative activity was calculated after standardization to the total protein content.

2.4 | Alizarin red s staining and quantification

The hASCs were cultured in PM or OM for 14 days and used for the mineralization assay. After fixation in 95% ethanol, the hASCs were stained with 1% Alizarin red s (ARS) staining solution (pH 4.2; Sigma-Aldrich) for 20 min at room temperature. To quantify mineralization levels, solutions obtained from the dissolved stainings using 100 mM cetylpyridinium chloride (Sigma-Aldrich) for 1 hr were measured by an EnSpire multimode plate reader (PerkinElmer, Waltham, MA) at 562 nm. ARS relative intensity was calculated after standardization to the total protein content.

2.5 | RNA extraction, reverse transcription, and quantitative real-time polymerase chain reaction

The total RNA was extracted with TRIzol reagent (Invitrogen, Carlsbad, CA) and reverse-transcribed into complementary DNA

with a reverse transcription system (Takara, Tokyo, Japan). Quantitative real-time polymerase chain reaction (qRT-PCR) was performed using the power SYBR green PCR master mix (Roche, Indianapolis, IN) and a 7500 real-time PCR detection system (Applied Biosystems, Foster City, CA). Glyceraldehyde-3-phosphate dehydrogenase (GAPDH) and U6 were used as internal controls for mRNAs and miR-137, respectively. The primer sequences are shown in Table 1. The $2^{-\Delta\Delta C_t}$ relative expression method was used to analyze the data.

2.6 | Western blot analysis

Total proteins were obtained with radioimmunoprecipitation assay (RIPA) lysis buffer (Sigma-Aldrich) and 2% protease inhibitor cocktail (Roche). Electrophoresis and transmembrane methods were applied as in the previous study (Jin et al., 2017). Primary antibodies against LSD1 (Cell Signaling Technology, Beverly, MA), BMP2 (Cell Signaling Technology), SMAD4 (Abcam, Cambridge, UK), runt-related transcription factor 2 (RUNX2; Cell Signaling Technology), and GAPDH (Cell Signaling Technology) were diluted to 1:1000 and incubated with the membranes at 4°C overnight. Secondary antibodies of horseradish peroxidase-conjugated goat anti-rabbit (Abcam) were diluted to 1:10,000 and incubated with the membrane at room temperature for 1 hr.

2.7 | Dual-luciferase report assay

Luciferase reporter assays were performed as in a previous study (Fan et al., 2016). In brief, LSD1 cDNA fragments containing the predicted potential miR-137 binding sites were amplified by PCR and cloned to pEZX-MT06 vector (GeneCopoeia, Guangzhou, China) to form a wild-type LSD1 (LSD1-WT) luciferase reporter plasmid. The mutation of miR-137 target sites in the LSD1 3' UTR was achieved by using a site-directed mutagenesis kit (SBS Genetech, Beijing, China) and a mutant-type LSD1 (LSD1-MT) luciferase reporter plasmid was obtained.

The hASCs were cultured in a 24-well plate and cotransfected with 100 nM negative control or miR-137 mimics, 1 μ g LSD1-WT or LSD1-MT luciferase reporter plasmid and lipofectamine 3000 (Invitrogen). After 48 hr, the dual-luciferase reporter assay system

(Promega) was used to detect luciferase activities. All luciferase activities were standardized to *Renilla* luciferase and were expressed relative to the basal activity.

2.8 | Heterotopic bone formation assay in vivo

This study was approved by the Institutional Animal Care and Use Committee of the Peking University Health Science Center (LA2019019) and all the animal experiments were confirmed to the institutional animal guidelines.

The hASCs transduced with lentiviruses (miR-137, anti-miR-137, and NC) were cultured in PM for 7 days before the in vivo study. The cells were collected and incubated with autsetting calcium phosphate cement (ACPC; Ruibang, Shanghai, China) at 37°C for 1 hr. The compounds were then implanted into the dorsum subcutaneous pockets of 5-week-old BALB/c homozygous nude (nu/nu) mice.

After 8 weeks of implantation, the specimens were collected and fixed in 10% neutral formaldehyde fixative. Soft X-ray pictures were captured under 22.0 kV, 22.5 mA at a distance of 20 cm using a Senograph 200D molybdenum-rhodium twin target X-ray device (GE, Fairfield, CT). After being decalcified in 10% ethylene diamine tetraacetic acid (pH 7.4) for 14 days, 4-mm-thick paraffin-embedded sections were stained with hematoxylin and eosin (HE) and Masson trichrome. IHC staining with primary antibodies against osteocalcin (OCN; Abcam) was also performed to evaluate osteogenesis. Finally, the tissue slices were observed and photographed under a light microscope (Olympus, Tokyo, Japan).

2.9 | Statistical analysis

SPSS Statistics 20.0 software (IBM, Armonk, NY) was used for statistical analysis. Data were shown as the mean \pm standard deviation of three independent experiments with error bars. A Student's *t* test or one-way analysis of variance combined with Tukey's test was used to compare two or multiple groups of data separately. A two-tailed value of $p < .05$ was considered statistically significant.

TABLE 1 Sequences of the primers used for qRT-PCR

	Forward primer (5' to 3')	Reverse primer (5' to 3')
LSD1	TGACCGGATGACTTCTCAAGA	GTTGGAGAGTAGCCTCAAATGTC
BMP2	GACTGCGGTCTCCTAAAGGTCTG	CTGGGGAAGCAGCAACGCTA
SMAD4	CCATCAGTCTGTCTGCTGCT	TGATGCTCTGTCTCGGGTAG
RUNX2	CCGCCTCAGTGATTTAGGGC	GGGTCTGTAATCTGACTCTGTCC
ALP	ATGGGATGGGTGTCTCCACA	CCACGAAGGGGAAGTCTGTC
OCN	CACTCCTCGCCCTATTGGC	CCCTCTGCTTGACACAAAG
GAPDH	GAAGGTGAAGGTCGGAGTC	GAAGATGGTGATGGGATTTTC
U6	CTCGCTTCGGCAGCACAA	AACGCTTCACGAATTTGCGT

Abbreviations: ALP, alkaline phosphatase; BMP2, bone morphogenetic protein 2; GAPDH, glyceraldehyde-3-phosphate dehydrogenase; LSD1, lysine-specific histone demethylase 1; OCN, osteocalcin; qRT-PCR, quantitative real-time polymerase chain reaction; RUNX2, runt-related transcription factor 2; SMAD4, mothers against decapentaplegic homolog 4

3 | RESULTS

3.1 | MiR-137 was downregulated during the osteogenic differentiation of hASCs

To investigate the involvement of miR-137 in the osteogenic differentiation of hASCs, we examined the expression of miR-137 during this process. From the relative expression of miR-137, a transient increase was observed on the first day, but it began to decrease significantly after 1 day and lasted for 14 days, the end point of our examination (Figure 1a). These results showed an overall decline in miR-137 expression during the osteogenic differentiation of hASCs.

3.2 | MiR-137 negatively affected the osteogenic differentiation of hASCs in vitro

To identify the role of miR-137 in the osteogenesis of hASCs, we transduced hASCs with miR-137, anti-miR-137, and NC lentiviruses. By calculating the percentage of GFP-positive cells, we evaluated the lentiviral transduction efficiency of hASCs was >90% (Figure 1b). The qRT-PCR analysis showed that the expression of miR-137 was more than 15-fold higher in the miR-137 group than in the NC group whereas the anti-miR-137 group showed a decline of over 70% (Figure 1c).

ALP and ARS staining were used to estimate the level of mineralization in vitro. Compared to the NC group, the anti-miR-137 group, respectively, displayed darker blue and more red calcium nodules in PM and OM. In contrast, lighter blue and fewer calcium nodules were observed in the miR-137 group (Figure 2a,b). The quantification of the two stainings showed increased levels of ALP activity and extracellular mineralization in the anti-miR-137 group, and contradictory results were obtained for the miR-137 group (Figure 2c,d). The relative expression of osteogenesis-associated genes, including RUNX2, ALP, and OCN, were significantly increased in the anti-miR-137 group and decreased in the miR-137 group compared with the NC group both in PM and OM (Figure 2e). Moreover, the protein expression of RUNX2, a critical transcription factor of osteogenesis, generated results similar to those of the qRT-PCR detection procedure (Figure 2f), demonstrating the negative role of miR-137 in the osteogenic differentiation of hASCs in vitro.

3.3 | MiR-137 negatively affected the osteogenic differentiation of hASCs in vivo

To further confirm whether miR-137 could negatively regulate the osteogenesis in vivo as it does in vitro, hASCs transduced with miR-137, anti-miR-137, and NC lentiviruses were loaded on ACPC scaffolds and implanted into the dorsal subcutaneous space of nude mice. The volume and mean density of the implantation specimens photographed by soft X-ray were significantly augmented in the anti-miR-137 group compared with the NC group whereas the miR-137 group was apparently diminished (Figure 3a,b).

HE staining results showed the largest amount of newly formed bone in the anti-miR-137 group, fewer osteoid tissues in the NC

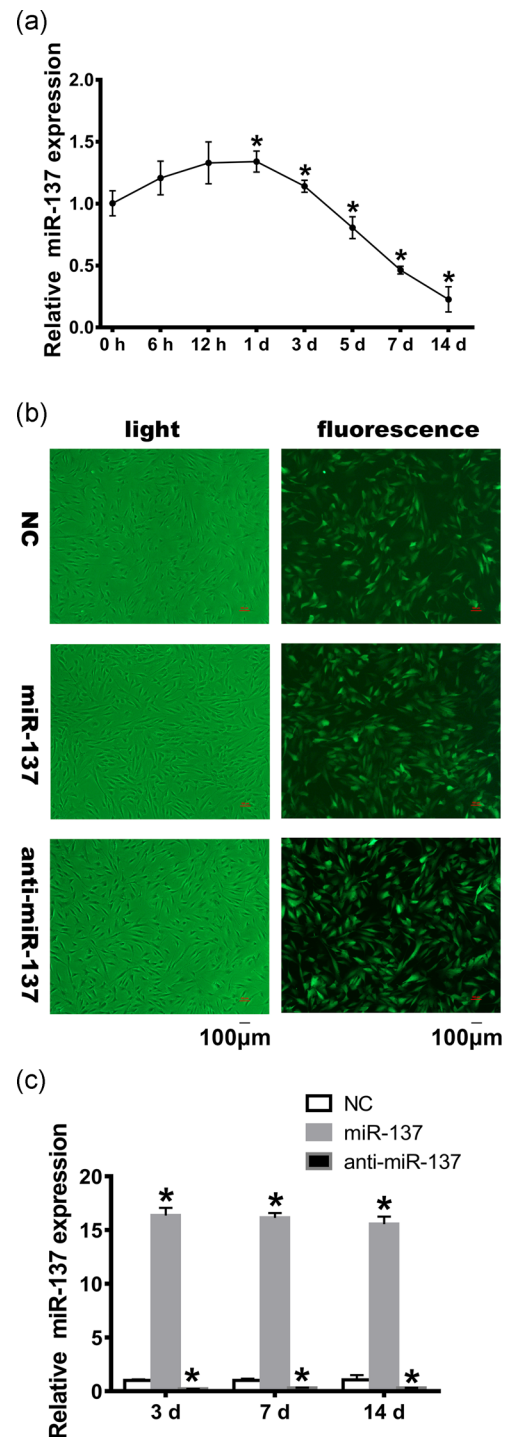
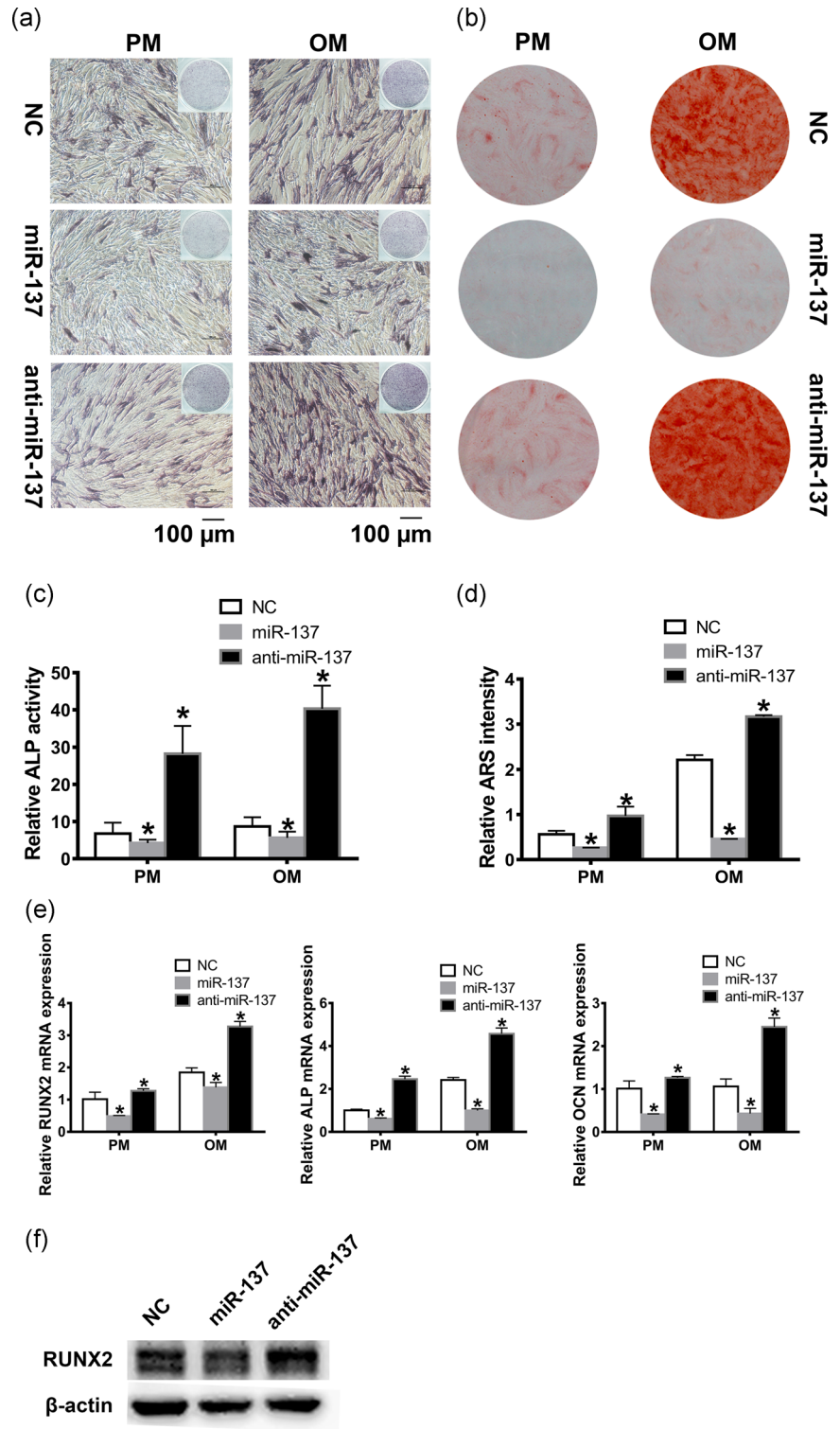


FIGURE 1 Expression of miR-137 during the osteogenic induction of hASCs and the efficiency of lentiviral transduction. (a) qRT-PCR analysis of miR-137 expression during the osteogenic differentiation of hASCs at different time points. Each bar represents the mean \pm SD for triplicate experiments. * $p < .05$ versus the 0 hr time point. (b) Microscopic images of GFP-positive hASCs after transduction under the ordinary and fluorescent light (scale bar = 100 μ m). (c) qRT-PCR analysis of miR-137 expression in transduced hASCs on 3, 7, and 14 days. Each bar represents the mean \pm SD for triplicate experiments. * $p < .05$ versus the NC group. anti-miR-137, miR-137 knockdown; GFP, green fluorescent protein; hASCs, human adipose-derived stem cells; miR-137, miR-137 overexpression; NC, negative control; qRT-PCR, quantitative real-time polymerase chain reaction; SD, standard deviation [Color figure can be viewed at wileyonlinelibrary.com]

FIGURE 2 MiR-137 negatively regulated the osteogenic differentiation of hASCs in vitro. (a) ALP staining of transduced hASCs cultured in PM or OM for 7 day (scale bar = 100 μ m). (b) ARS staining of transduced hASCs cultured in PM or OM for 14 days. (c) ALP quantification on 7 days. (d) ARS quantification on 14 days. (e) qRT-PCR analysis of RUNX2, ALP, and OCN expression in transduced hASCs cultured in PM or OM. (f) Western blot analysis of RUNX2 in transduced hASCs. Each bar represents the mean \pm SD for triplicate experiments. * p < .05 versus the NC group. ALP, alkaline phosphatase; anti-miR-137, miR-137 knockdown; ARS, alizarin red s; hASCs: human adipose-derived stem cells; OCN, osteocalcin; OM, osteogenic medium; PM, proliferation medium; miR-137, miR-137 overexpression; NC, negative control; qRT-PCR, quantitative real-time polymerase chain reaction; RUNX2: runt-related transcription factor 2 [Color figure can be viewed at wileyonlinelibrary.com]



group, and scarcely any detectable bone formation in the miR-137 group. Masson trichrome staining displayed more collagen fiber bundles arranged compactly in the anti-miR-137 group than in other two groups whereas the lowest levels of collagen deposition were observed in the miR-137 group. Moreover, IHC staining for OCN indicated that a large number of brown stained granules were widely distributed in hASCs of the anti-miR-137 group whereas the NC group included fewer and the miR-137 group hardly contained any

stained granules in cells (Figure 3c). Taken together, miR-137 could negatively regulated the osteogenesis of hASCs in vivo.

3.4 | MiR-137 positively regulated the expression of LSD1

Studies have reported that LSD1 is a target gene of miR-137 in several cell lines (Althoff et al., 2013; Chen et al., 2017; J. Q. Sun

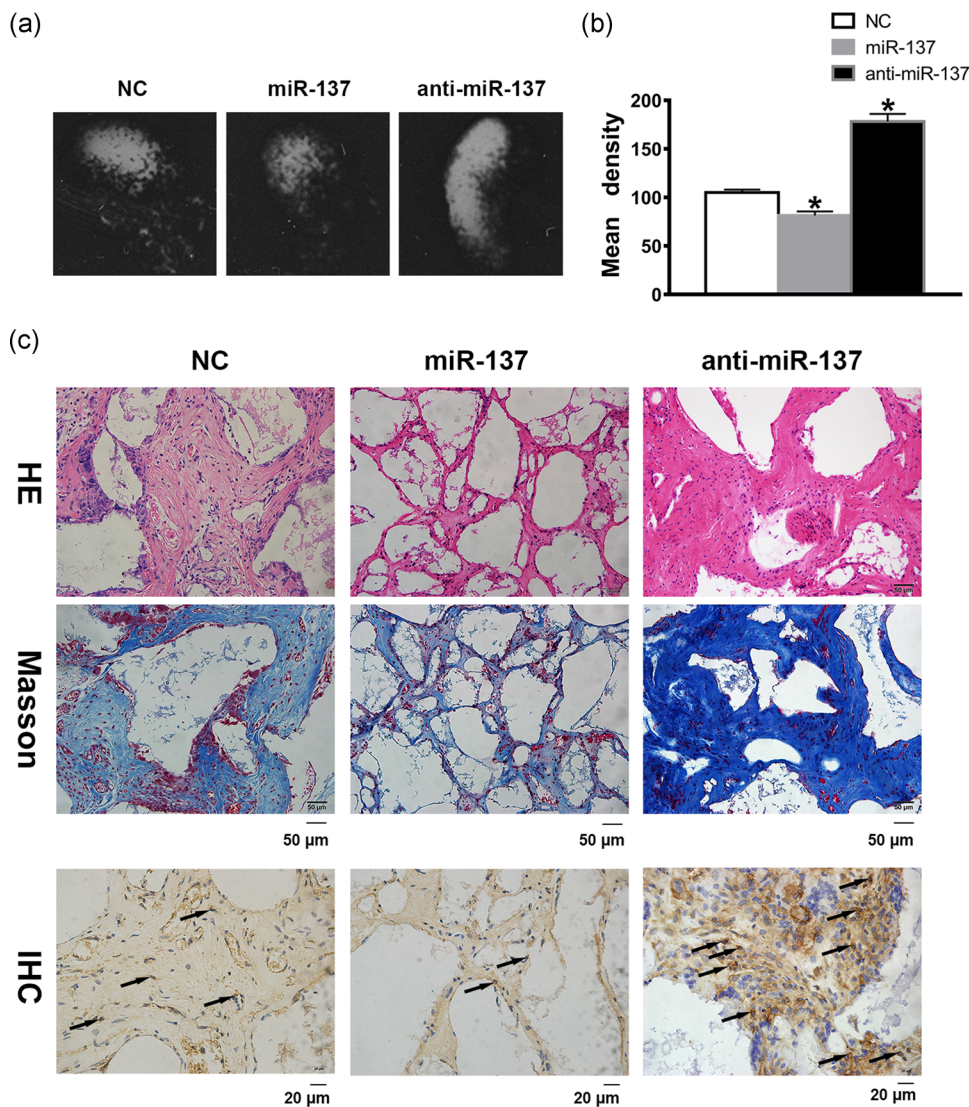


FIGURE 3 MiR-137 attenuated the heterotopic bone formation of hASCs in vivo. (a) Soft X-ray photograph of hASC-ACPC complexes implanted into nude mice for 8 weeks. (b) Relative grayscale analysis of the specimens generated with the ImageJ software. Each bar represents the mean \pm SD for triplicate experiments. * $p < .05$ versus the NC group. (c) Histological assessment of ectopic bone formation: HE staining (scale bar = 50 μ m), Masson trichrome staining (scale bar = 50 μ m) and IHC staining for OCN (scale bar = 20 μ m), dark-brown granules in cells denoting OCN positive staining were partially marked with black arrows. ACPC, autsetting calcium phosphate cement; anti-miR-137, miR-137 knockdown; hASCs, human adipose-derived stem cells; HE, hematoxylin and eosin; IHC, immunohistochemical; OCN, osteocalcin; NC, negative control; miR-137, miR-137 overexpression [Color figure can be viewed at wileyonlinelibrary.com]

et al., 2011; Zhang et al., 2017; W. Zhang et al., 2018), so we tried to determine whether miR-137 had influence on LSD1 expression and through this way it regulated the osteogenic differentiation of hASCs. However, the expression of LSD1 adapted with changes in miR-137 at the mRNA and protein levels in our study. In other words, miR-137 knockdown repressed the expression of LSD1, and overexpression of miR-137 induced LSD1 expression in hASCs (Figure 4a,b).

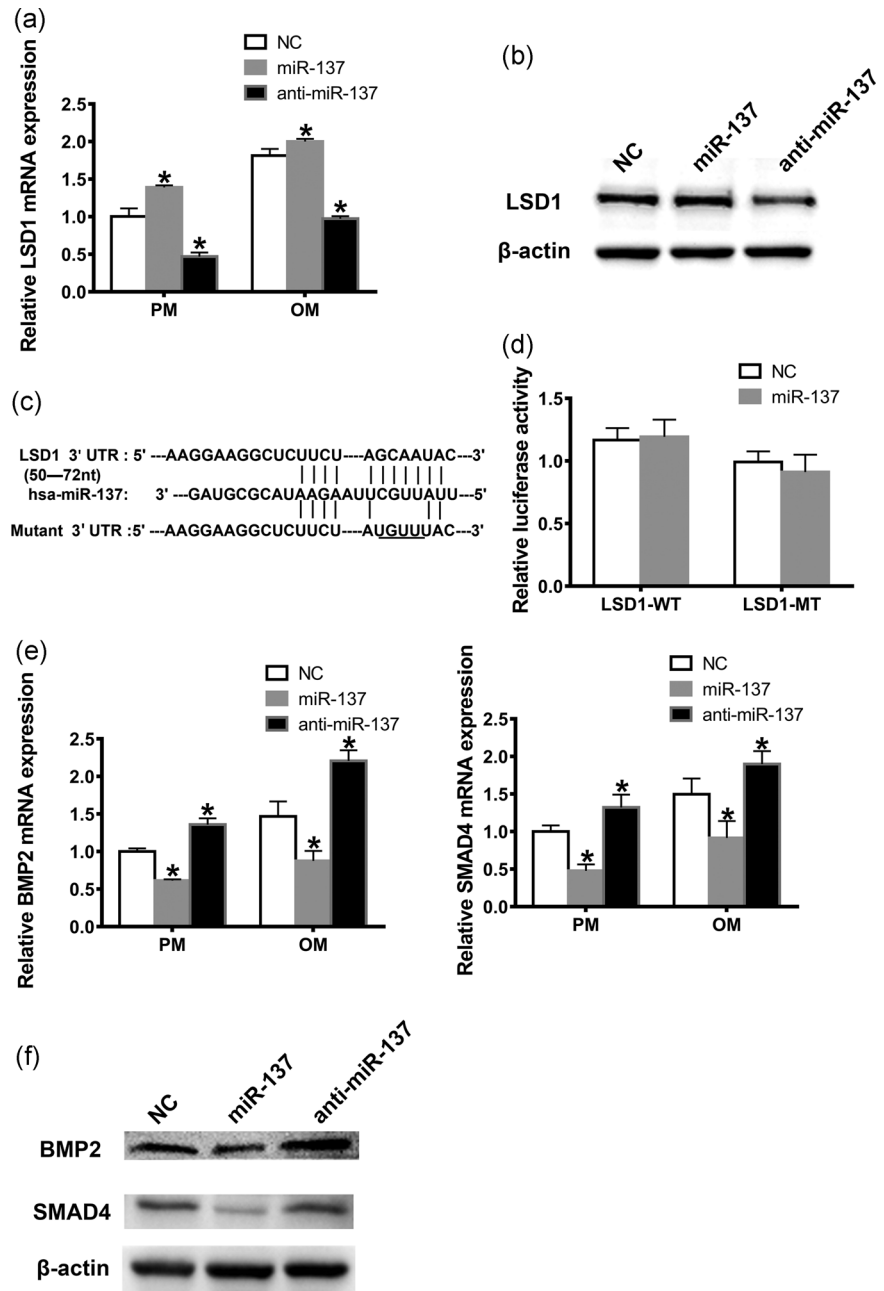
To further confirm our results, a dual-luciferase reporter assay was performed, but the relative luciferase activity analysis did not show any significant differences between the NC group and miR-137 group whether LSD1-WT or LSD1-MT luciferase reporter plasmid was used (Figure 4c,d). In contrast to the results reported

in other cell lines, our data indicated that instead of being directly targeted by miR-137 in hASCs, LSD1 was positively regulated by miR-137, which might be mediated by some other unknown genes. Thus, in this way, LSD1 was involved in the osteogenic regulation of miR-137.

3.5 | MiR-137 negatively regulated the BMP2-SMAD4 pathway

Because BMP signaling is a canonical pathway in the osteogenic differentiation, we further investigated whether it could be affected by miR-137 in this process. BMP7 was once identified as a target gene of miR-137 in non-small-cell lung cancer cells (Y. R. Yang et al.,

FIGURE 4 MiR-137 positively regulated LSD1, and suppressed the BMP2-SMAD4 pathway. qRT-PCR (a) and western blot analysis (b) analysis of the effects of miR-137 on LSD1 expression. (c) Predicted binding sites of miR-137 in the 3' UTR of LSD1-WT mRNA (the underlined section denoted mutated base sequences in the 3' UTR of LSD1-MT); (d) Luciferase activity of cells in the LSD1-WT or LSD1-MT group. qRT-PCR (e) and western blot analysis (f) analysis of the effects of miR-137 on BMP2 and SMAD4 expression. Each bar represents the mean \pm SD for triplicate experiments. * $p < .05$ versus the NC group. BMP2, bone morphogenetic protein 2; LSD1: lysine-specific histone demethylase 1; LSD1-WT, wild-type LSD1; LSD1-MT, mutant-type LSD1; OM, osteogenic medium; SMAD4, mothers against decapentaplegic homolog 4; PM, proliferation medium; 3' UTR, 3' untranslated region; miR-137: miR-137 overexpression; NC, negative control; anti-miR-137, miR-137 knockdown; qRT-PCR, quantitative real-time polymerase chain reaction; SD, standard deviation



2015), but our qRT-PCR analysis showed that BMP7 expression was increased in the miR-137 group whereas decreased in the anti-miR-137 group, which was consistent with the alterations of miR-137 expression in hASCs (Figure S1). However, the mRNA and protein expressions of BMP2 and its downstream gene SMAD4 were upregulated in the anti-miR-137 group whereas being significantly downregulated in the miR-137 group (Figure 4e,f). These results showed that miR-137 could negatively regulate BMP2 and SMAD4 expression, suggesting that miR-137 knockdown might promote the osteogenesis of hASCs by stimulating the BMP2-SMAD4 pathway.

To further ascertain whether the downregulation of BMP2 observed was based on direct binding by miR-137, we performed a dual-luciferase reporter assay and found that BMP2 was not a target gene of miR-137 in hASCs (Figure S2). These results prompted us

that some other molecules or signals might mediate the modulation of miR-137 in BMP2 expression.

3.6 | LSD1 knockdown increased the expression of BMP2 and SMAD4

To identify relationships between the downstream genes of miR-137 validated above in the osteogenic regulation of hASCs, we transduced hASCs with anti-LSD1 and NC lentiviruses. The relative mRNA expression of LSD1 resulted in an over 80% reduction in the anti-LSD1 group compared with the NC group (Figure 5a). Protein level underwent a significant decrease in the anti-LSD1 group as well (Figure 5b).

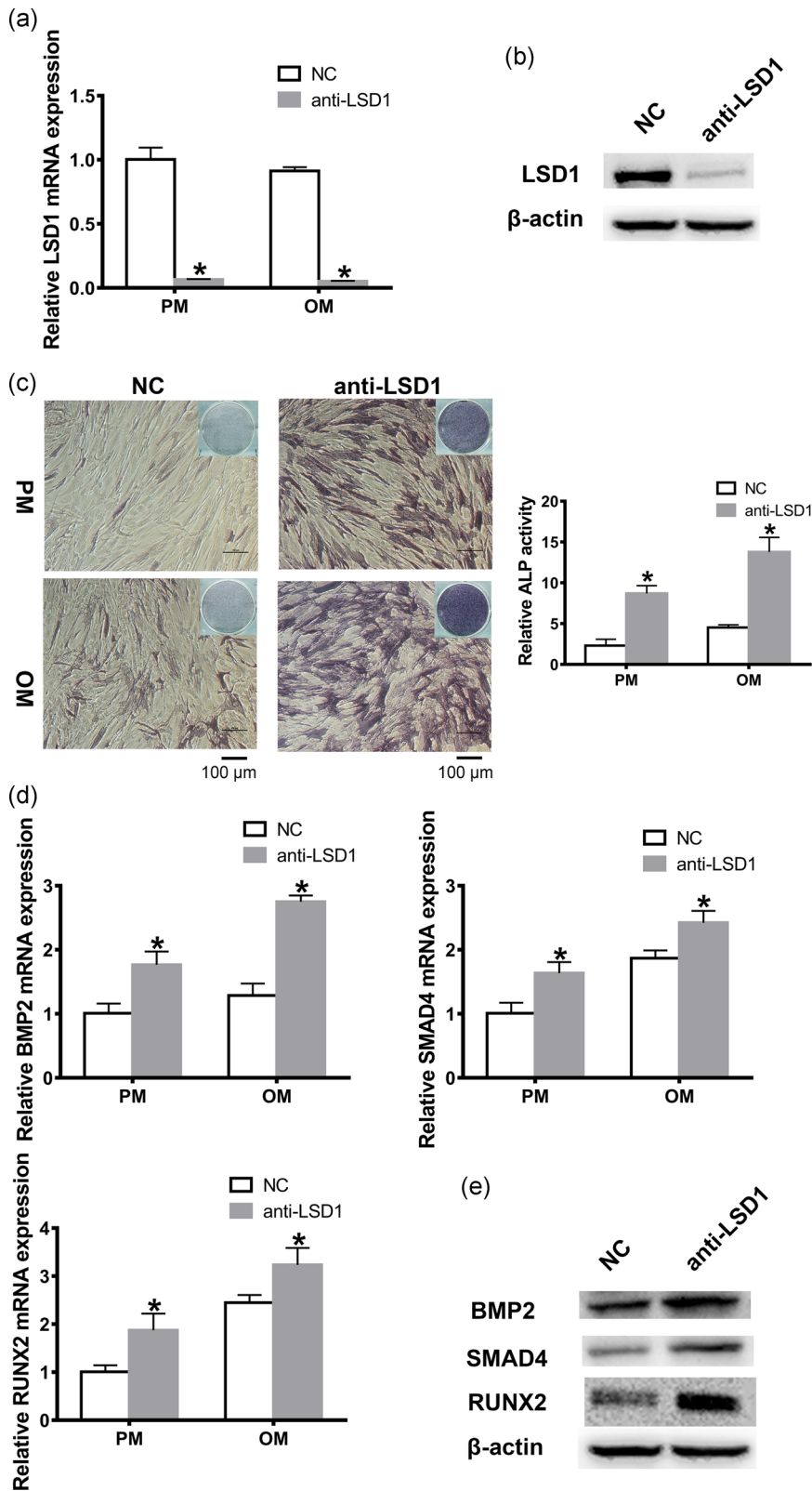


FIGURE 5 LSD1 knockdown activated the BMP2-SMAD4 pathway. qRT-PCR (a) and western blot analysis (b) analysis of LSD1 expression in hASCs after anti-LSD1 lentivirus transduction. (c) ALP staining and quantification of hASCs after LSD1 knockdown in the PM and OM group (scale bar = 100 μ m). qRT-PCR (d) and western blot analysis (e) analysis of BMP2, SMAD4, and RUNX2 expression after LSD1 knockdown. Each bar represents the mean \pm SD for triplicate experiments. * $p < .05$ versus the NC group. anti-LSD1, LSD1 knockdown; ALP, alkaline phosphatase; BMP2, bone morphogenetic protein 2; SMAD4, mothers against decapentaplegic homolog 4; hASCs, human adipose-derived stem cells; LSD1, lysine-specific histone demethylase 1; miR-137, miR-137 overexpression; NC, negative control; OM, osteogenic medium; PM, proliferation medium; qRT-PCR, quantitative real-time polymerase chain reaction; RUNX2, runt-related transcription factor 2; SD, standard deviation [Color figure can be viewed at wileyonlinelibrary.com]

In concert with the above results showing that miR-137 positively regulated LSD1 whereas negatively regulating osteogenesis, the osteogenic promotion effect observed after LSD1 knockdown was reaffirmed by ALP staining and quantification (Figure 5c). In addition, LSD1 knockdown upregulated the expression of BMP2, SMAD4, and

RUNX2 at the mRNA and protein levels (Figure 5d,e). Taken together, these results revealed that in coordination with miR-137 knockdown, LSD1 knockdown could also stimulate the BMP2-SMAD4 pathway and initiate the osteogenic differentiation, suggesting that miR-137 knockdown could activate the BMP2-SMAD4

pathway and osteogenic differentiation through the downregulation of LSD1 independently or dependently.

4 | DISCUSSION

MiR-137 has been identified as a tumor repressor in many studies (Chen et al., 2018; Huang et al., 2018; N. Lv et al., 2018; W. Zhang et al., 2018), and its function research on the proliferation and differentiation of stem cells is mainly in neural differentiation. MiR-137 could induce the differentiation of adult mouse neural stem cells, mouse oligodendrogloma-derived stem cells and human glioblastoma multiforme-derived stem cells and induce the cell cycle arrest of glioblastoma multiforme (Silber et al., 2008). Additionally, miR-137 controlled the dynamics between proliferation and differentiation of the neural stem cells by forming a regulatory loop with nuclear receptor TLX and LSD1 (J. Q. Sun et al., 2011). In mouse ESCs, miR-137 targeted Klf4 and Tbx3 and accelerated neural differentiation (Jiang, Ren, & Nair, 2013). However, no research on the role of miR-137 in osteogenic differentiation has been reported. Though we observed a transient increase in miR-137 expression on the first day during the osteogenic induction of hASCs, a significant decrease was observed from Day 1 and that lasted to the end of our examination. The overall decline in miR-137 expression indicated that miR-137 might play a negative role in this process. As it has been demonstrated that miR-137 can suppress proliferation and migration in several types of cells (Bi, Xia, & Wang, 2018; Pan, Li, Huang, & Zhang, 2017; Q. Zhang et al., 2018), the transitory increase in miR-137 expression observed in the early phase of osteogenesis might relate to the inhibition of cell proliferation and the initiation of subsequent osteogenic differentiation.

The hASCs in vitro with miR-137 knockdown showed increased ALP activity, extracellular matrix mineralization, and osteogenesis-associated gene expression of RUNX2, ALP, and OCN. Moreover, a significantly higher degree of ectopic bone formation was confirmed in vivo after implanting of hASCs in the anti-miR-137 group and ACPC compounds. Conversely, overexpression of miR-137 exhibited impaired osteogenic capacities in the above experiments. Therefore, the combination of our in vitro and in vivo experiments verified the negative effects of miR-137 on the osteogenic differentiation of hASCs, manifesting that miR-137 knockdown promoted the osteogenic differentiation of hASCs whereas overexpression of miR-137 attenuated this biological process.

LSD1 has been reported as a target gene of miR-137 in several studies (Althoff et al., 2013; Chen et al., 2017; J. Q. Sun et al., 2011; X. Zhang et al., 2017; W. Zhang et al., 2018). Our previous studies also demonstrated that the genetic or chemical inhibition of LSD1 could promote the osteogenic differentiation of MSCs (Ge et al., 2014; Lv et al., 2016). Thus, we hypothesized that miR-137 could regulate LSD1 expression, through which it might affect the osteogenic differentiation of hASCs. However, we confirmed that LSD1 was not negatively regulated by miR-137 as observed in other studies, as the alterations of LSD1 expression were found to be

consistent with miR-137 overexpression/knockdown at both the mRNA and protein levels. Furthermore, a dual-luciferase reporter assay validated the conclusion that LSD1 was not a target gene of miR-137 in hASCs, coinciding with our qRT-PCR and western blot analysis results. We attributed these conflicting results to the diverse biological properties of different cell lines, and further research is needed to reveal the intermediary regulator acting between miR-137 and LSD1 in the osteogenic differentiation of hASCs.

Numerous studies have substantiated the vital role of BMP signaling in skeletal development and bone formation. As members of the BMP family, BMP2 and BMP7 were the first to be identified by their ability to promote osteogenesis (Deng et al., 2008; Salazar, Gamer, & Rosen, 2016), and FDA-approved recombinant human BMP2 and BMP7 homodimers have been shown to impart benefits in clinical trials (Bi et al., 2018). In non-small-cell lung cancer cells, miR-137 inhibits cell migration and invasion by targeting the 3' UTR of BMP7 directly (Y. R. Yang et al., 2015). However, our data presented consistent changes in BMP7 expression with miR-137 alterations. We conjectured that like the promotion effect on LSD1, miR-137 might positively regulate BMP7 expression depending on some unascertained intermediary regulators. The various biological properties and distinct involved pathways in different cell lines might contribute to our contrary results. Considering sharing certain receptors with BMP7 in the signaling pathway (Suzuki et al., 1997), BMP2 might also be regulated by miR-137. As expected, our study verified that miR-137 could repress the expression of BMP2 and its downstream gene SMAD4, but unlike the direct binding on the 3' UTR of BMP7 in cancer cell lines, BMP2 was indirectly repressed by miR-137 in hASCs. Due to the regulation of specific intermediate signaling molecules, BMP2 and BMP7 could probably be oppositely regulated by miR-137. BMP7 was found to impair the osteogenic differentiation of bone marrow derived MSCs and the extent of enhanced mineralization by BMP2 was diminished when BMP2 was replaced or supplemented by BMP7 (Wongwitwichot & Kaewsrichan, 2017). Another study also showed the variability of BMP7 in the osteogenic regulation. The hASCs with BMP2 treatment for 15 min induced osteogenic differentiation, whereas BMP7 stimulated a chondrogenic phenotype (Knippenberg, Helder, Zandieh Doulabi, Wuisman, & Klein-Nulend, 2006). These data suggested that BMP7 was not a singular lineage determinant and could act as a bidirectional regulator in osteogenesis depending on certain conditions. Our study supported that miR-137 knockdown could promote the osteogenesis of hASCs by activating the BMP2-SMAD4 pathway, prompting that there might exist unknown molecules mediating the modulation of miR-137 in BMP2 expression.

It has been reported that a rhodium (III)-based inhibitor of LSD1 promoted the amplification of BMP2 gene promoters in prostate cancer cells (Yang et al., 2017), and LSD1 deficiency could result in increased BMP2 expression in osteoblasts and enhanced bone formation (J. Sun et al., 2018). In this study, we confirmed that LSD1 knockdown enhanced the osteogenic differentiation of hASCs and upregulated the expression of BMP2 and SMAD4. Similar to miR-137 knockdown, LSD1 knockdown could promote the osteogenesis

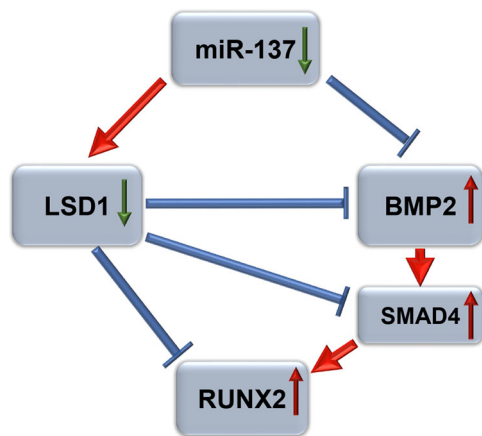


FIGURE 6 Schematic of the LSD1/BMP2/SMAD4 signaling network involved in the osteogenic regulation of miR-137 in hASCs. MiR-137 knockdown could repress LSD1, activate the BMP2-SMAD4 pathway, and finally enhance RUNX2 expression. Moreover, downregulated LSD1 generated through miR-137 knockdown promoted the BMP2-SMAD4 pathway and RUNX2 expression. Therefore, the LSD1/BMP2/SMAD4 signaling network coregulated the osteogenic differentiation of hASCs. BMP2, bone morphogenetic protein 2; hASCs, human adipose-derived stem cells; LSD1, lysine-specific histone demethylase 1; RUNX2, runt-related transcription factor 2; SMAD4, mothers against decapentaplegic homolog 4 [Color figure can be viewed at wileyonlinelibrary.com]

of hASCs by stimulating the BMP2-SMAD4 pathway as well. In summary, besides activating the BMP2-SMAD4 pathway independently, miR-137 knockdown could regulate this pathway by downregulating LSD1 as well, and other molecules may also participate in the regulation of LSD1 by miR-137. Therefore, we proposed a coregulatory network composed of LSD1, BMP2, SMAD4 and other unknown signaling molecules, contributing to the regulation of miR-137 in the osteogenic differentiation of hASCs.

In conclusion, miR-137 knockdown could promote the osteogenic differentiation of hASCs via the LSD1/BMP2/SMAD4 signaling network (Figure 6). Our study elucidated some of the mechanisms that underlie this biological process and revealed a potential therapeutic target for hASC-based bone tissue engineering.

ACKNOWLEDGMENTS

This study was financially supported by grants from the National Natural Science Foundation of China (81700937), and the Project for Culturing Leading Talents in Scientific and Technological Innovation of Beijing (Z171100001117169).

CONFLICT OF INTEREST

The authors declare that there are no conflicts of interest.

AUTHOR CONTRIBUTIONS

X. M. conducted experiments and wrote the manuscript; Y. W., Y. D., and Y. Z. assisted to do experiments and collected data; H. L.,

L. L., Y. L. analyzed data; Y. Z. and C. F. designed the concept, wrote a manuscript, provided financial support, and approved manuscript.

REFERENCES

- Althoff, K., Beckers, A., Oderskym, A., Mestdag, P., Köster, J., Bray, I. M., ... Schulte, J. H. (2013). MiR-137 functions as a tumor suppressor in neuroblastoma by downregulating KDM1A. *International Journal of Cancer*, 133(5), 1064–1073.
- Ambros, V. (2004). The functions of animal microRNAs. *Nature*, 431, 350–355.
- Behr, B., Tang, C., Germann, G., Longaker, M. T., & Quarto, N. (2011). Locally applied VEGFA increases the osteogenic healing capacity of human adipose derived stem cells by promoting osteogenic and endothelial differentiation. *Stem Cells*, 29(2), 286–296.
- Bi, W., Liu, Y., Guo, J., Lin, Z., Liu, J., Zhou, M., ... Wu, G. (2018). All-trans retinoic acid inhibits heterodimeric bone morphogenetic protein 2/7-stimulated osteoclastogenesis, and resorption activity. *Cell and Bioscience*, 8, 48–60.
- Bi, W. P., Xia, M., & Wang, X. J. (2018). MiR-137 suppresses proliferation, migration and invasion of colon cancer cell lines by targeting TCF4. *Oncology Letters*, 15(6), 8744–8748.
- Cai, Q., Zheng, P., Ma, F., Zhang, H., Li, Z., Fu, Q., ... Sun, Y. (2019). MicroRNA-224 enhances the osteoblastic differentiation of hMSCs via Rac1. *Cell Biochemistry and Function*, 37(2), 62–71.
- Chen, F., Luo, N., Hu, Y., Li, X., & Zhang, K. (2018). MiR-137 suppresses triple-negative breast cancer stemness and tumorigenesis by perturbing BCL11A-DNMT1 interaction. *Cellular Physiology and Biochemistry*, 47(5), 2147–2158.
- Chen, L., Wang, X., Huang, W., Ying, T., Chen, M., Cao, J., & Wang, M. (2017). MicroRNA-137 and its downstream target LSD1 inversely regulate anesthetics-induced neurotoxicity in dorsal root ganglion neurons. *Brain Research Bulletin*, 135, 1–7.
- Dai, Z., Jin, Y., Zheng, J., Liu, K., Zhao, J., Zhang, S., ... Sun, Z. (2019). MiR-217 promotes cell proliferation and osteogenic differentiation of BMSCs by targeting DKK1 in steroid-associated osteonecrosis. *Biomedicine & Pharmacotherapy*, 109, 1112–1119.
- Deng, Z. L., Sharff, K. A., Tang, N., Song, W. X., Luo, J., Luo, X., ... He, T. C. (2008). Regulation of osteogenic differentiation during skeletal development. *Frontiers in Bioscience-Landmark*, 13, 2001–2021.
- Fan, C., Jia, L. F., Zheng, Y. F., Jin, C. Y., Liu, Y. S., Liu, H., & Zhou, Y. S. (2016). MiR-34a promotes osteogenic differentiation of human adipose-derived stem cells via the RBP2/NOTCH1/CYCLIN D1 coregulatory network. *Stem Cell Reports*, 7(2), 236–248.
- Ge, W. S., Liu, Y. S., Chen, T., Zhang, X., Lv, L. W., Jin, C. Y., ... Zhou, Y. S. (2014). The epigenetic promotion of osteogenic differentiation of human adipose-derived stem cells by the genetic and chemical blockade of histone demethylase LSD1. *Biomaterials*, 35(23), 6015–6025.
- Huang, B., Huang, M., & Li, Q. (2018). MiR-137 suppresses migration and invasion by targeting EZH2-STAT3 signaling in human hepatocellular carcinoma. *Pathology, Research and Practice*, 214(12), 1980–1986.
- Jiang, K., Ren, C., & Nair, V. D. (2013). MicroRNA-137 represses Klf4 and Tbx3 during differentiation of mouse embryonic stem cells. *Stem Cell Research*, 11(3), 1299–1313.
- Jin, C. Y., Zheng, Y. F., Huang, Y. P., Liu, Y. S., Jia, L. F., & Zhou, Y. S. (2017). Long non-coding RNA MIAT knockdown promotes osteogenic differentiation of human adipose-derived stem cells. *Cell Biology International*, 41, 33–41.
- Knippenberg, M., Helder, M. N., Zandieh Doulabi, B., Wuisman, P. I., & Klein-Nulend, J. (2006). Osteogenesis versus chondrogenesis by BMP-2 and BMP-7 in adipose stem cells. *Biochemical and Biophysical Research Communications*, 342(3), 902–908.

- Liu, Y., Zhao, Y., Zhang, X., Chen, T., Zhao, X., Ma, G., & Zhou, Y. (2013). Flow cytometric cell sorting and in vitro pre-osteoinduction are not requirements for in vivo bone formation by human adipose-derived stromal cells. *PLOS One*, 8(2), e56002.
- Liu, Y., Zhou, Y., Feng, H., Ma, G., & Ni, Y. (2008). Injectable tissue-engineered bone composed of human adipose-derived stromal cells and platelet-rich plasma. *Biomaterials*, 29(23), 3338–3345.
- Lv, L. W., Ge, W. S., Liu, Y. S., Lai, G. Y., Liu, H., Li, W. Y., & Zhou, Y. S. (2016). Lysine-specific demethylase 1 inhibitor rescues the osteogenic ability of mesenchymal stem cells under osteoporotic conditions by modulating H3K4 methylation. *Bone Research*, 4, 16037.
- Lv, N., Hao, S., Luo, C., Abukiwan, A., Hao, Y., Gai, F., ... He, D. (2018). MiR-137 inhibits melanoma cell proliferation through downregulation of GLO1. *Science China-Life Sciences*, 61(5), 541–549.
- Massagué, J., Seoane, J., & Wotton, D. (2005). Smad transcription factors. *Genes & Development*, 19(23), 2783–2810.
- vanMeurs, J. B., Boer, C. G., Lopez-Delgado, L., & Riancho, J. A. (2019). Role of epigenomics in bone and cartilage disease. *Journal of Bone and Mineral Research*, 34(2), 215–230.
- Pan, J., Li, K., Huang, W., & Zhang, X. (2017). MiR-137 inhibited cell proliferation and migration of vascular smooth muscle cells via targeting IGFBP-5 and modulating the mTOR/STAT3 signaling. *PLOS One*, 12(10), e0186245.
- Perillo, B., Ombra, M. N., Bertoni, A., Cuozzo, C., Sacchetti, S., Sasso, A., ... Avvedimento, E. V. (2008). DNA oxidation as triggered by H3K9me2 demethylation drives estrogen-induced gene expression. *Science*, 319(5860), 202–206.
- Rosen, V. (2009). BMP2 signaling in bone development and repair. *Cytokine & Growth Factor Reviews*, 20(5–6), 475–480.
- Salazar, V. S., Gamer, L. W., & Rosen, V. (2016). BMP signalling in skeletal development, disease and repair. *Nature Reviews Endocrinology*, 12(4), 203–221.
- Shi, Y., Lan, F., Matson, C., Mulligan, P., Whetstine, J. R., Cole, P. A., ... Shi, Y. (2004). Histone demethylation mediated by the nuclear amine oxidase homolog LSD1. *Cell*, 119(7), 941–953.
- Shu, B., Zhang, M., Xie, R., Wang, M., Jin, H., Hou, W., ... Chen, D. (2011). BMP2, but not BMP4, is crucial for chondrocyte proliferation and maturation during endochondral bone development. *Journal of Cell Science*, 124(20), 3428–3440.
- Silber, J., Lim, D. A., Petritsch, C., Persson, A. I., Maunakea, A. K., Yu, M., ... Hodgson, J. G. (2008). MiR-124 and miR-137 inhibit proliferation of glioblastoma multiforme cells and induce differentiation of brain tumor stem cells. *BMC Medicine*, 6, 14–30.
- Sun, G. Q., Ye, P., Murai, K., Lang, M. F., Li, S. X., Zhang, H., ... Shi, Y. H. (2011). MiR-137 forms a regulatory loop with nuclear receptor TLX and LSD1 in neural stem cells. *Nature Communications*, 2, 529–548.
- Sun, J., Ermann, J., Niu, N., Yan, G., Yang, Y., Shi, Y., & Zou, W. (2018). Histone demethylase LSD1 regulates bone mass by controlling WNT7B and BMP2 signaling in osteoblasts. *Bone Research*, 6, 14–25.
- Suzuki, A., Kaneko, E., Ueno, N., & Hemmati-Brivanlou, A. (1997). Regulation of epidermal induction by BMP2 and BMP7 signaling. *Developmental Biology*, 189(1), 112–122.
- Tang, J. Z., Lin, X., Zhong, J. Y., Xu, F., Wu, F., Liao, X. B., ... Yuan, L. Q. (2019). MiR-124 regulates the osteogenic differentiation of bone marrow-derived mesenchymal stem cells by targeting Sp7. *Molecular Medicine Reports*, 19(5), 3807–3814.
- Wang, C. G., Liao, Z., Xiao, H., Liu, H., Hu, Y. H., Liao, Q. D., & Zhong, D. (2019). LncRNA KCNQ1OT1 promoted BMP2 expression to regulate osteogenic differentiation by sponging miRNA-214. *Experimental and Molecular Pathology*, 107, 77–84.
- Wongwitwichot, P., & Kaewsrirachan, J. (2017). Osteogenic differentiation of mesenchymal stem cells is impaired by bone morphogenetic protein 7. *Advances in Medical Sciences*, 62(2), 266–272.
- Yang, C., Liu, X., Zhao, K., Zhu, Y., Hu, B., Zhou, Y., ... Zou, D. (2019). MiRNA-21 promotes osteogenesis via the PTEN/PI3K/Akt/HIF-1 α pathway and enhances bone regeneration in critical size defects. *Stem Cell Research & Therapy*, 10(1), 65–75.
- Yang, C., Wang, W., Liang, J. X., Li, G., Vellaisamy, K., Wong, C. Y., ... Leung, C. H. (2017). A rhodium (III)-based inhibitor of lysine-specific histone demethylase 1 as an epigenetic modulator in prostate cancer cells. *Journal of Medicinal Chemistry*, 60(6), 2597–2603.
- Yang, Y. R., Li, Y. X., Gao, X. Y., Zhao, S. S., Zang, S. Z., & Zhang, Z. Q. (2015). MicroRNA-137 inhibits cell migration and invasion by targeting bone morphogenetic protein-7 (BMP7) in non-small cell lung cancer cells. *International Journal of Clinical and Experimental Pathology*, 8(9), 10847–10853.
- Yu, L., Han, M., Yan, M., Lee, J., & Muneoka, K. (2012). BMP2 induces segment-specific skeletal regeneration from digit and limb amputations by establishing a new endochondral ossification center. *Developmental Biology*, 372(2), 263–273.
- Zhang, J., He, J., & Zhang, L. (2018). The down-regulation of microRNA-137 contributes to the up-regulation of retinoblastoma cell proliferation and invasion by regulating COX-2/PGE2 signaling. *Biomedicine & Pharmacotherapy*, 106, 35–42.
- Zhang, Q., Guo, B., Hui, Q., Chang, P., & Tao, K. (2018). MiR-137 inhibits proliferation and metastasis of hypertrophic scar fibroblasts via targeting pleiotrophin. *Cellular Physiology and Biochemistry*, 49(3), 985–995.
- Zhang, W., Chen, J. H., Shan, T. J., Aguilera-Barrantes, I., Wang, L. S., Huang, H. M., ... Huang, Y. W. (2018). MiR-137 is a tumor suppressor in endometrial cancer and is repressed by DNA hypermethylation. *Laboratory Investigation*, 98(11), 1397–1407.
- Zhang, X., Zhang, X., Yu, B., Hu, R., & Hao, L. (2017). Oncogene LSD1 is epigenetically suppressed by miR-137 overexpression in human non-small cell lung cancer. *Biochimie*, 137, 12–19.

SUPPORTING INFORMATION

Additional supporting information may be found online in the Supporting Information section.

How to cite this article: Ma X, Fan C, Wang Y, et al. MiR-137 knockdown promotes the osteogenic differentiation of human adipose-derived stem cells via the LSD1/BMP2/SMAD4 signaling network. *J Cell Physiol*. 2019;1–11.

<https://doi.org/10.1002/jcp.29006>